

© 2011 Geological Society of America

using the numerical model, GEOCLIM, to evaluate the impact of paleogeography and rock weathering on $\text{CO}_{2\text{atm}}$ level and climate (Figs. 1 and 2). The advantage of the GEOCLIM model, compared to previous modeling, is its ability to account explicitly for the role of plate motion on the long-term geochemical (through the weathering of silicate rocks) and climatic evolution of the Earth surface (Donnadieu et al., 2006b). These two factors have been proved to influence significantly the weatherability of the continents and to affect the carbon cycle for more recent time periods (Kump et al., 1999; Dessert et al., 2001; Dupré et al., 2003; Donnadieu et al., 2004; Donnadieu et al., 2006b; Royer 2006; Goddérès et al., 2008). Only the multimillion-year background $\text{CO}_{2\text{atm}}$ level (and coeval climate) is calculated, without considering short-term perturbations of the global carbon cycle, such as, for instance, the Hirnantian glacial climax.

MODEL DESCRIPTION AND FORCING FACTORS

GEOCLIM Description

The GEOCLIM model couples a 3D atmospheric general circulation model (the fast ocean-atmosphere model [FOAM] GCM; Jacob, 1997) to a model of the biogeochemical cycles of carbon and alkalinity (the coupled model of biogeochemical cycles and climate [COMBINE] model,

Goddérès and Joachimski, 2004; Donnadieu et al., 2006b; Goddérès et al., 2008). A full description of the GEOCLIM model was published by Donnadieu et al. (2006b; see the references therein). The modeling procedure is based on the concept of the long-term stability of the global climate, which requires the balance between CO_2 consumption by continental silicate rock weathering and solid Earth CO_2 degassing (Walker et al., 1981). First of all, FOAM computes the climatic parameters, temperature, and runoff, which allow the calculation of the atmospheric CO_2 sink by continental weathering by COMBINE. Indeed, the CO_2 consumption by silicate rock weathering is assumed to depend on air temperature and continental runoff (Dessert et al., 2003; Oliva et al., 2003). It is calculated using the climatic field from the GCM with a spatial resolution of 7.5° longitude \times 4.5° latitude. Then, fixing the source of CO_2 through solid Earth degassing, a numerical feedback loop between FOAM and COMBINE is run until the sink through weathering equilibrates the prescribed degassing. At the same time, the model reaches a steady-state $p\text{CO}_{2\text{atm}}$ for each continental configuration. This coupled model allows thus the coeval calculation of the $\text{CO}_{2\text{atm}}$ level and of the climate. Note that to spare computation time, the coupling between the FOAM GCM and the COMBINE model employs look-up tables from a catalog of climate simulations (Donnadieu et al., 2006b). Because there is no consensus about the Earth degassing rate for the past 200 million years where

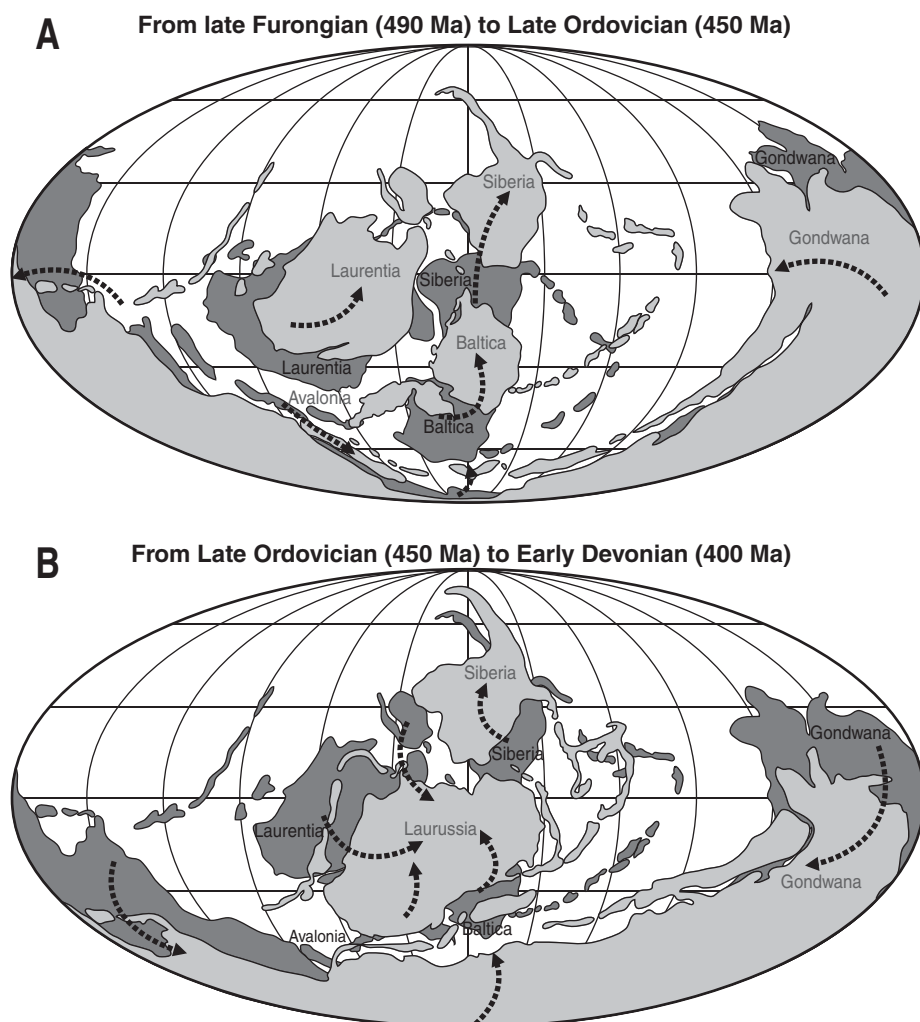


Figure 1. Main continental movements between the late Furongian (dark gray) and the Late Ordovician (light gray) (A), and the Late Ordovician (dark gray) and the Early Devonian (light gray) (B), based on the paleogeographic reconstructions of Blakey (2007) included in the model GEOCLIM (a climate model coupled to a biogeochemical model). Dashed arrows show approximately the drift direction for each continental mass.

data are available (see Kerrick, 2000 and Donnadieu et al., 2006b), we do not feel that any constraint can be put on this source flux for the Paleozoic where a single reconstruction is available (Gaffin, 1987). Thus this rate is kept constant at its present-day value, assuming that the present-day CO_2 consumption by weathering is equal to the CO_2 degassing (6.8×10^{12} moles $\text{CO}_2 \cdot \text{yr}^{-1}$) (Gaillardet et al., 1999).

Five time slices have been simulated (stages dated according to Gradstein et al., 2004): Furongian (Stage 10; 490 Ma), Middle Ordovician (early Dapingian; 470 Ma), Late Ordovician (middle Katian; 450 Ma), Llandovery (late Telychian; 430 Ma), and Early Devonian (late Emsian; 400 Ma). For each continental configuration, major topographical barriers have been reconstructed and land surface type is set to rocky desert (because the land plants were not well developed on continents until the Early Devonian; Wellman et al., 2003). According to stellar evolution models, the solar luminosity is thought to increase, from 95.4% of

its present-day value ($1368 \text{ W} \cdot \text{m}^{-2}$) in the Furongian (late Cambrian) to 96.7% in the Early Devonian (Gough, 1981; Crowley et al., 1991).

For each time slice, the model is run until steady-state is reached, meaning that $\text{CO}_{2\text{atm}}$ and climate are constant. The atmospheric CO_2 production by Earth degassing F_{outgas} and the total consumption by silicate weathering are then balanced (Walker et al., 1981; Godd  ris et al., 2003):

$$\sum_j A_j (\phi_{\text{volc}}) f_{\text{volc}}(T_j, \text{runoff}_j) + \sum_j A_j (\phi_{\text{sil}} - \phi_{\text{volc}}) f_{\text{shield}}(T_j, \text{runoff}_j) = F_{\text{outgas}} \quad (1)$$

The two terms on the left side are, respectively, the CO_2 consumption by volcanic rock weathering and by other silicate rocks. The sums extend over all continental grid elements. The term A_j is the area of a continental grid

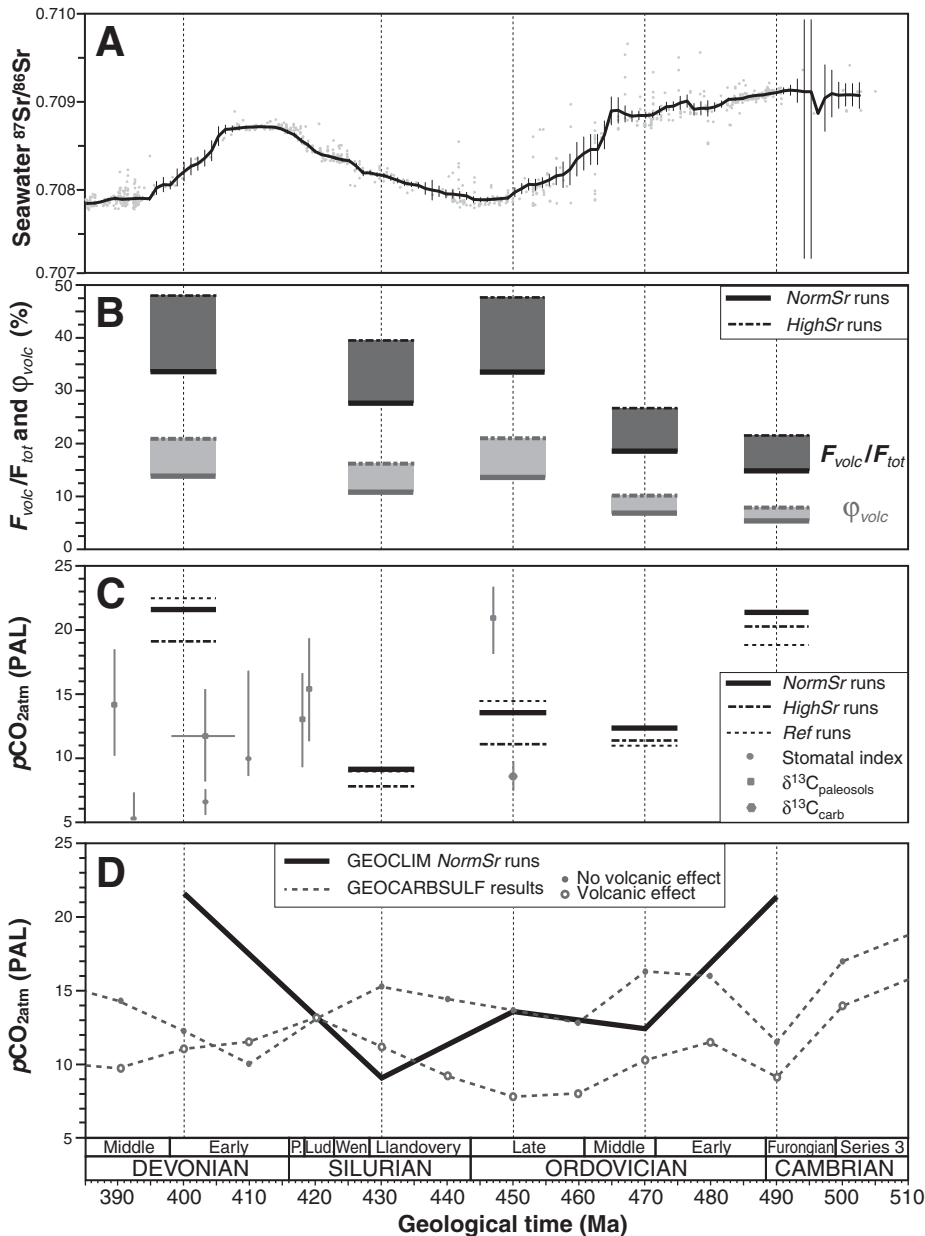


Figure 2. (A) $^{87}\text{Sr}/^{86}\text{Sr}$ secular variations and averaged curves with confidence interval (error bars) based on the database of Veizer et al. (1999). (B) Calculated proportions of outcropping basic volcanic rocks (ϕ_{volc} , gray bars) for the NormSr and HighSr simulations; the Ref simulation values being at 11% according to D  rr et al. (2005); and calculated CO_2 consumption through the weathering of the basic volcanic rocks (F_{volc}) in proportion to the total CO_2 consumption by continental silicate rock (F_{tot}) weathering (black bars) for the NormSr and HighSr simulations (values obtained with the Ref simulations being relatively constant around $28.5 \pm 0.5\%$). (C) Modeled $p\text{CO}_{2\text{atm}}$ values (preindustrial atmospheric level [PAL]); thick dark boxes based on the NormSr and HighSr simulations; thin dashed lines based on the Ref simulations; and reconstructed values based on stomatal index $\delta^{13}\text{C}_{\text{carb}}$ and $\delta^{13}\text{C}_{\text{paleosols}}$; Yapp and Poeths, 1996; Patzkowsky et al., 1997; Royer, 2006. (D) Modeled $p\text{CO}_{2\text{atm}}$ values (PAL) with GEOCLIM (black thick line) and comparison with GEOCARBSULF from Berner (2006) (gray lines) at with (o) or without (x) term for volcanic rock weathering. Horizontal error bars in (B) and (C) represent the age error of the paleogeographic maps (assumed to be ± 5 m. y.).

element j , n being the total number of these elements. The term ϕ_{sil} is the fraction of each grid element covered by old silicate rock outcrop (which will be weathered after extrusion and not right after formation), and ϕ_{volc} is the fraction occupied by fresh volcanic rocks (which are directly exposed to the weathering as soon as they are formed). Today, the fraction of the outcropping silicate rocks is fixed at 71% for each continental grid element (Dürr et al., 2005). This value is held constant in our experiments. There is no explicit distribution of the lithology in the GEOCLIM model, because there is no sufficient constraint in the distant past, except for the well-studied zones (e.g., North America and Europe). We assume thus that each continental grid element has the same proportion of outcropping volcanic and shield rocks (including plutonic and sedimentary siliciclastic rocks) for a given time slice in the past. This proportion is then calculated as a function of time, based on the recorded $^{87}\text{Sr}/^{86}\text{Sr}$ ratio as described below (Veizer et al., 1999). The functions f_{shield} and f_{volc} are the climatic dependences of the chemical weathering of old silicate outcrops and fresh volcanic rocks, respectively (Dessert et al., 2003; Oliva et al., 2003).

Volcanic Rock Weathering

The long-term fluctuations of the $^{87}\text{Sr}/^{86}\text{Sr}$ isotopic record (10^7 yr) have been interpreted for a long time as relative changes in the contribution of continental weathering (providing high-radiogenic strontium with high $^{87}\text{Sr}/^{86}\text{Sr}$ values) versus seawater hydrothermal interactions (providing low-radiogenic strontium with low $^{87}\text{Sr}/^{86}\text{Sr}$ values). However, this simple interpretation was proved wrong because it implies too large fluctuations in the ocean-atmosphere carbon reservoir (Goddéris and François, 1995; Kump and Arthur, 1997). It has been proposed that long-term $^{87}\text{Sr}/^{86}\text{Sr}$ fluctuations primarily reflected changes in the isotopic composition of the continental source rocks exposed to weathering as it has been demonstrated for the Cenozoic history of the seawater $^{87}\text{Sr}/^{86}\text{Sr}$ and the Himalayan uplift (Goddéris and François, 1995; Galy et al., 1999).

During the early Paleozoic, the decrease of seawater $^{87}\text{Sr}/^{86}\text{Sr}$ isotopic ratio by about 0.001 from the Furonian to the Late Ordovician evidenced by Veizer et al. (1999; Fig. 2A) has been interpreted as reflecting a rising contribution of the weathering of fresh volcanic rocks to the oceanic strontium reservoir (Berner, 2006b; Young et al., 2009; Buggisch et al., 2010). Similarly, it has been recently suggested that weathering of fresh low-radiogenic volcanic rocks from the Taconic and Kazakhstan arcs could have induced a rapid decrease in the seawater $^{87}\text{Sr}/^{86}\text{Sr}$ during the Ordovician (Young et al., 2009). This process might have been responsible for the cooling between the late Middle Ordovician and the Llandovery (Kump et al., 2000; Young et al., 2009).

Therefore we estimate the relative proportion of fresh volcanic rocks outcropping on the continents by solving the following equation for ϕ_{volc} , the fraction of each grid element covered with fresh volcanic rocks:

$$\sum_j \frac{A_j \cdot (\phi_{sil} - \phi_{volc}) \cdot f_{shield}(T_j, runoff_j) \cdot (r_{shield} - r_{oc})}{9.43 + r_{shield}} + \sum_j \frac{A_j \cdot \phi_{volc} \cdot f_{volc}(T_j, runoff_j) \cdot (r_{volc} - r_{oc})}{9.43 + r_{volc}} + \frac{F_{Sr}^{carb} \cdot (r_{carb} - r_{oc})}{9.43 + r_{carb}} + \frac{F_{Sr}^{MOR} \cdot (r_{MOR} - r_{oc})}{9.43 + r_{MOR}} = 0. \quad (2)$$

The term ϕ_{volc} is assumed to be the same for each grid element, but it changes from one simulated time slice to another. Indeed, r_{oc} is the

$^{87}\text{Sr}/^{86}\text{Sr}$ of seawater as recorded in carbonate sediments for each time slice (Veizer et al., 1999; Fig. 2A). The term r_{shield} is the $^{87}\text{Sr}/^{86}\text{Sr}$ ratio of shield rocks. It is calculated at 0.716 for the early Paleozoic, assuming an initial Rb/Sr ratio of 0.0981, and held constant in all simulations. This value is assumed to be valid for siliciclastic rocks. The term r_{MOR} is the isotopic ratio of deep-sea fresh basalts (0.70302 for the Ordovician time, using the $^{87}\text{Sr}/^{86}\text{Sr}_{BAB1}$ at 0.69897) (Papanastassiou and Wasserburg, 1969). The term r_{volc} is the volcanic rock $^{87}\text{Sr}/^{86}\text{Sr}$. Two values are tested. We first assume that this ratio is equal to the mantle value of 0.70302 (*NormSr* run). However, continental basalts may display much higher isotopic ratios due to crustal contamination (e.g., 0.705–0.709 for Taconic tephra; Samson, 1996). Therefore, additional simulations are performed with r_{volc} fixed at 0.707 (*HighSr* run), being intermediate between the Taconic extremes.

The strontium isotopic cycle is calibrated using the present-day Sr fluxes taken from the literature (Wallmann, 2001a). Solving equation (2) for ϕ_{volc} implies that the oceanic strontium isotopic budget is balanced for each time slice, an assumption consistent with the exploration of the multimillion-year mean state of the biogeochemical cycles performed here. In comparison to the calculations of Young et al. (2009), our present method uses the FOAM GCM to estimate the link between CO_2 atm, air temperature and runoff, and the strontium and CO_2 consumption fluxes through continental silicate weathering fluxes for each continental grid element (Donnadieu et al., 2006b).

Finally, the GEOCLIM model is run, for each investigated time slice, (1) with the proportions of shield and volcanic rocks held at their present-day value (60% and 11%, respectively; Dürr et al., 2005) (*Ref* run) and (2) with their estimated proportions based on equation (2) (*NormSr* and *HighSr* run) as explained above. The impact of the volcanic rock weathering and plate motion on the CO_2 consumption and the climatic evolution can thus be discriminated.

Paleogeographic Forcing of the Carbon Cycle in the Early Paleozoic

Numerous ocean-ridge systems were developed during the breakup of the supercontinent Rodinia reducing the oceanic basin volume since the late Proterozoic. Hence, continents were progressively flooded and sea level reached its maximum in the Late Ordovician (Haq and Schutter, 2008). Continents were largely dispersed in a 60° belt south of the paleoequator in the Furonian. Gondwana shifted to a position in which North Africa was centered over the South Pole (Fig. 1), while Laurentia, Avalonia, Siberia, and Baltica slowly moved towards low latitudes during the Late Ordovician (Cocks and Torsvik, 2002; Blakey, 2007). Then Gondwana rotated clockwise and moved toward the tropical latitude; the South Pole migrated successively from north Argentina-Paraguay during Silurian to Namibia during the Early Devonian. Laurussia, resulting from the Silurian amalgamation of Baltica-Avalonia with Laurentia rapidly drifted southward whilst undergoing counterclockwise rotation (Fig. 1). The continental location in the warm and humid tropical zone could have enhanced runoff rates and CO_2 consumption through rock weathering (Boucot and Gray, 2001). The two supercontinents (Gondwana and Laurussia) were mainly located in the Southern Hemisphere; only a few microcontinents, parts of Laurussia, and Siberia were located in the Northern Hemisphere (Cocks and Torsvik, 2002).

The GEOCLIM model explicitly uses the geographic reconstructions proposed by one of the authors (R.B.). These paleogeographic reconstructions are in relative agreement on the global plate-motion directions and timing through the early Paleozoic with reconstructions proposed by others (see McKerrow and Scotese, 1990; Cocks and Torsvik, 2002; Stampfli and Borel, 2002; Scotese, 2004; Blakey, 2007). Therefore our study takes

into account the general consensus in paleogeographic changes even if only one reconstruction is tested here (Fig. 1).

RESULTS AND DISCUSSION

Volcanic Rock Weathering

Calculated proportion of low-radiogenic volcanic rocks (*NormSr* run) increases from 5.4% of the total continental surface in the Furongian to 13.5% in the Late Ordovician. This proportion then slightly decreases in the Silurian (10.5%) and increases again in the Early Devonian (13.5%) (Table 1; Fig. 2B, lower bond values). The opposite trend is observed for the high-radiogenic shield rocks, but their calculated values maintain an average of eight times those of volcanic rocks on continents during the study interval. The contribution of volcanic rocks weathering to the total CO_2 consumption by silicate rock dissolution increases from the Furongian (less than 15%) to the Late Ordovician (33%) (*NormSr* run). The last value is close to the present-day contribution of 30% (Dessert et al., 2003; Dupré et al., 2003, and references therein). These trends are confirmed by the *HighSr* simulations, with an increasing impact of the volcanic rocks weathering (Table 1; Fig. 2B, upper bond values). Indeed, the larger isotopic ratio of rocks used in *HighSr* simulations (when compared to *NormSr* runs) requires a larger input of low-radiogenic rocks to keep the budget in equilibrium. Moreover, the consumption of $\text{CO}_{2\text{atm}}$ through the weathering of volcanic rocks is maximal during the Late Ordovician (Fig. 2B).

Variations in calculated proportions of outcropping shield and volcanic rocks through time are in agreement with the geological record. Our calculation of a high fraction of shield rocks during the Furongian–Middle Ordovician interval is supported by recorded occurrence of several orogenic events between the Cambrian Series 3 (middle Cambrian) and the Early Ordovician, (1) on Baltica (e.g., Finnmarkian orogeny; Sturt et al., 1978), (2) on Laurentia (Penobscot orogeny; Hibbard et al., 2002), and (3) on Gondwana (Grampian, Ocloyic, Rio Doce, and Ross orogenies; Campos Neto and Figueiredo, 1995; Veveers, 2004; Thomas and Astini, 2007). Calculated rise of outcropping volcanic rocks is consistent with the increase of the record of K-bentonites and of the probable volcanic complexes (e.g., Famatinian, Sayan, and Taconic arcs) during the Ordovician (Min et al., 2001; Cocks and Torsvik, 2002; Huff, 2008; Young et al., 2009). The proportion of volcanic rocks decreases in favor of the shield rocks in the Llandovery (Fig. 2B). This trend is sustained by the net decline of volcanic records and the increasing number of orogenic events during the Late Ordovician–Silurian (e.g., Acatean, Altai, Benambran, Shelvian, and Taconic orogenies; Cocks and Torsvik, 2002; Dewey, 2005; Thomas and Astini, 2007; Ganis and Wise, 2008). However, a reversed trend during the Early Devonian shows a second increase in the proportions of outcropping volcanic rocks (Fig. 2B) consistent with the geological volcanic record (Francis, 1988; Demoux et al., 2009).

Atmospheric CO_2

Levels of $p\text{CO}_{2\text{atm}}$ calculated with the *NormSr* simulation fall from around 21 PAL in the Furongian down to about 12 and 14 PAL in the Middle and Late Ordovician, respectively (Fig. 2C). Levels continue to decrease until the Llandovery (9 PAL). Then calculated atmospheric CO_2 rises dramatically to 22 PAL in the Early Devonian. *HighSr* simulation $\text{CO}_{2\text{atm}}$ levels show a shift about 1.5 PAL lower than *NormSr* simulation levels, except in the Late Ordovician (about 2.5 PAL). *Ref* simulation $\text{CO}_{2\text{atm}}$ levels (performed with constant fresh volcanic rock outcrop) are lower than those calculated with the *NormSr* and *HighSr* simulations in the late Furongian–Middle Ordovician, and mainly higher for the rest of

TABLE 1. MAIN PARAMETERS OF THE GEOCLIM MODEL FOR THE SELECTED TIME SLICES

TABLE 1. MAIN PARAMETERS OF THE GEOLIM MODEL FOR THE SELECTED TIME SLICES																								
Age (Ma)	$^{87}\text{Sr}/^{86}\text{Sr}$ ratio	Solar constant ($\text{W}\cdot\text{m}^{-2}$)	Continental surface (10^6 km^2)	φ_{volc} (%)			$p\text{CO}_2$ (PAL)			$f_{\text{volc}}^{\text{shield}}$ (10^{12} moles $\text{CO}_2\cdot\text{yr}^{-1}$)			$f_{\text{volc}}^{\text{volc}}$ (10^{12} moles $\text{CO}_2\cdot\text{yr}^{-1}$)			$f_{\text{volc}}^{\text{atm}}$ (10^{12} moles $\text{CO}_2\cdot\text{yr}^{-1}$)			Runoff ($\text{cm}\cdot\text{yr}^{-1}$)			Continental temperature ($^{\circ}\text{C}$)		
				NormSr	HighSr	Ref	NormSr	HighSr	Ref	NormSr	HighSr	Ref	NormSr	HighSr	Ref	NormSr	HighSr	Ref	NormSr	HighSr	Ref	NormSr	HighSr	Ref
400	0.707904	1323	121.9	13.5	21.4	22	19	23	4.52	3.52	4.83	2.28	3.28	1.97	33.9	32.4	34.4	15.8	14.6	16.2	15.8	14.6	16.2	
430	0.708273	1319	113.9	10.6	16.5	9	8	9	4.92	4.10	4.84	1.88	2.70	1.96	37.8	36.5	37.7	13.5	12.4	13.4	13.5	12.4	13.4	
450	0.707900	1316	108.6	13.5	21.4	14	11	14	4.53	3.54	4.86	2.27	3.26	1.94	37.2	35.5	37.7	13.9	12.6	14.3	13.9	12.6	14.3	
470	0.708839	1313	136.0	6.8	15.4	12	11	11	5.53	4.97	4.83	1.27	1.83	1.97	32.2	31.4	31.2	13.3	12.7	12.6	13.3	12.7	12.6	
490	0.709075	1305	128.6	5.4	8.1	21	20	19	5.78	5.33	4.86	1.02	1.47	1.94	31.8	31.2	30.5	16.2	15.8	15.3	16.2	15.8	15.3	

Note: The functions $f_{\text{volc}}^{\text{shield}}$ and $f_{\text{volc}}^{\text{volc}}$ represent the calculated CO_2 consumption via shield and volcanic rock weathering. The $^{87}\text{Sr}/^{86}\text{Sr}$ ratio was calculated from a mobile average over 8 m.y., based on the dataset published by Veizer et al. (1999). The solar constant value refers to the trend published in Gough (1981), compared to the modern solar constant value (1368 $\text{W}\cdot\text{m}^{-2}$). The continental surface is calculated based on the paleogeographic maps of Blakey (2007). The other geochemical model inputs are equivalent to those published by Donnadieu et al. (2006b). PAL — preindustrial atmospheric level

Note: The functions f_{volc} and f_{volc} represent the calculated CO_2 consumption via shield and volcanic rock weathering. The $^{87}\text{Sr}/^{86}\text{Sr}$ ratio was calculated from a mobile average over 8 m.y., based on the dataset published by Veizer et al. (1999). The solar constant value refers to the trend published in Gough (1981), compared to the modern solar constant value (1368 Wm^{-2}). The continental surface is calculated based on the paleogeographic maps of Blakey (2007). The other geochemical model inputs are equivalent to those published by Donnadieu et al. (2006b). PAL—preindustrial atmospheric level.

the period (Table 1 and Fig. 2C). *Ref* simulation values especially differ from the *NormSr* simulations for the Furongian and the Middle Ordovician (being at 19 and 11 PAL, respectively). The most obvious result is the onset of a low CO_2 time window between the Middle Ordovician and the Llandovery. The timing of this lower CO_2 window is roughly consistent with the maximum extension of the glacial period. However, the model is unable to clearly distinguish the short-term perturbation of the Hirnantian event from the Late Ordovician cooling trend, due to its low time-scale resolution.

Our modeled atmospheric $p\text{CO}_2$ values are in between the two reconstructed values for the Late Ordovician (14–20 PAL; estimations based on $\delta^{13}\text{C}_{\text{carb}}$ and $\delta^{13}\text{C}_{\text{paleosols}}$; Yapp and Poths, 1996; Patzkowsky et al., 1997; Fig. 2C). Our $p\text{CO}_2$ values also fall roughly in the range of the previously modeled values for the Middle Ordovician–Llandovery (Bernier, 2006a, 2006b [Fig. 2D]; Crowley and Baum, 1995; Bernier and Kothavala, 2001; and see for the single Late Ordovician: Gibbs et al., 1997; Poussart et al., 1999; Herrmann et al., 2004a, 2004b; Young et al., 2009). The modeled value of 22 PAL for the Early Devonian is largely higher than the earlier published values modeled (10–14 PAL) (Bernier, 1998, 2006b; Bernier and Kothavala, 2001) and inferred from $p\text{CO}_2$ proxies (7–15 PAL; paleosols and stomatal index; see Royer, 2006) (Fig. 2C). The absence of land plants impact on the weathering of the continents in our model could be partly responsible for this difference.

Our results can be compared in more details to the results of another model of the global biogeochemical cycles for the Middle Ordovician–Llandovery (GEOCARBSULF; Bernier, 2006a, 2006b, 2008). Our modeled $p\text{CO}_2$ values are similar to those computed by GEOCARBSULF with no volcanic rock weathering effect for the Furongian–Late Ordovician period and closer to those computed by GEOCARBSULF with an imposed volcanic rock weathering factor during the Llandovery (Fig. 2D). However, both models simulated two different trends for the same period. GEOCLIM predicts a time window of low $p\text{CO}_{2\text{atm}}$, while GEOCARBSULF predicts an overall decreasing trend. GEOCARBSULF also predicts a slight increase in $\text{CO}_{2\text{atm}}$ levels from the Late Ordovician to the Silurian, while GEOCLIM calculates a further decrease (Fig. 2D).

It may be fruitful to explore why models are producing different results because model output cannot be readily compared without consideration of the model structures. GEOCARBSULF calculates the long-term evolution of the cycles of carbon and sulfur (and their exchanges between rocks and the superficial system) (see Bernier, 2006a, 2006b for complete description). It uses several fixed nondimensional parameters to simulate the impact of physical erosion, runoff, and plant evolution on silicate weathering (Bernier and Kothavala, 2001; Bernier, 2006a). GEOCARBSULF computes the $p\text{CO}_{2\text{atm}}$ based on the calculation of the global mean silicate weathering (which is not spatially resolved) using global runoff and temperature (Bernier, 2006a), although off-line GCM simulations are also used to roughly evaluate the impact of paleogeography on those global climatic parameters. It also accounts for the effect of the organic carbon burial on the $\text{CO}_{2\text{atm}}$ pressure (see Bernier, 2004, for complete description).

GEOCLIM only accounts for a few forcing functions (e.g., $^{87}\text{Sr}/^{86}\text{Sr}$, paleogeography), but computes a process-based method with a physical description of the online coupling between CO_2 , climate, and continental configurations for each time slice, whereas GEOCARBSULF accounts for more processes controlling the silicate weathering, but the method is global and mainly phenomenological. Considering these differences in the model structures and even if in both cases, the account of the volcanic rock weathering draws down the calculated $p\text{CO}_2$, differences in the modeled trends could be explained by (1) the explicit and physically based consideration in GEOCLIM of the consequences of paleogeographic changes through time and (2) the computation of the weathering fluxes with a spatial resolution. Indeed, weathering rates are dependent on climate through

nonlinear mathematical relationships (Dessert et al., 2003; Oliva et al., 2003). As a consequence, the use of mean global temperature and mean global runoff in GEOCARBSULF may induce non-negligible biases in the estimation of the impact of the paleogeographic setting on the Earth system evolution.

Our modeled U-shaped CO_2 trend is due to the response of the geochemical cycles and climate to the slow drift of the continental plates and to the fluctuating area of fresh volcanic rocks, which are being weathered on the continents. The *Ref* simulation, performed with a constant area of volcanic rocks for all time slices, can be used to discriminate both factors (Fig. 2C). The difference between the *Ref* and *NormSr* (or *HighSr*) simulations increases from the Furongian to the Late Ordovician (Fig. 2C). The model thus predicts an increasing impact of the volcanic rock weathering during this time interval, with a peak of 33% of the total CO_2 consumption through silicate weathering in the Late Ordovician. This effect is even more important with the *HighSr* configuration, which could suggest that further investigations about the $^{87}\text{Sr}/^{86}\text{Sr}$ value of the volcanic rocks are required. Nevertheless, despite small differences in the $\text{CO}_{2\text{atm}}$ level, the U-shaped curve suggesting the existence of a lower CO_2 time window from the Middle Ordovician to the Llandovery is also predicted in the *Ref* simulation. Varying outcrop of fresh volcanic rocks is thus a non-negligible contributor to the long-term $\text{CO}_{2\text{atm}}$ changes, but it is clearly not the main driver in our simulations. The main driver is the plate motion. This factor has been previously proved crucial in its impact on the fluctuations of the $\text{CO}_{2\text{atm}}$ level through the Mesozoic (Donnadieu et al., 2006b; Godd  ris et al., 2008).

The following scenario can thus be drawn from the numerical simulations of the early Paleozoic. The northward drift of Laurentia, Avalonia, Baltica, and Siberia is responsible for the $\text{CO}_{2\text{atm}}$ drawdown between 500 and 470 Ma (Fig. 1A). Indeed, in response to the motion of these four continental blocks, the continental runoff to the ocean increases substantially in the ITCZ (Fig. 3A). This increase promotes CO_2 consumption through continental weathering; consequently, $p\text{CO}_{2\text{atm}}$ decreases from 21 to 13 PAL. By contrast, the continental water discharge declines during the Late Ordovician around 10  N and displays a pattern similar to that of the Furongian (Fig. 3A and Table 1), although $p\text{CO}_{2\text{atm}}$ levels remain as low as those of the Middle Ordovician (11–14 PAL; Fig. 2C). Reduction of continental areas (Table 1) due to a major transgressive trend (Haq and Schutter, 2008), particularly pronounced in the ITCZ (Fig. 3C), should have induced lower continental weathering rates at 450 Ma than at 470 Ma (Table 1), thereby increasing $\text{CO}_{2\text{atm}}$ levels. But this effect is partly counterbalanced by the increasing outcrop area of fresh volcanic rocks (evidenced by the decrease in the seawater $^{87}\text{Sr}/^{86}\text{Sr}$ record), and consequently by a more efficient $\text{CO}_{2\text{atm}}$ consumption through their faster weathering.

The Late Ordovician interval is the only time window when the CO_2 consumption by fresh volcanic rock weathering plays a significant role (Table 1). After the Late Ordovician, the continental configuration again controls the calculated CO_2 evolution with the progressive amalgamation of Baltica and Avalonia first and later with Laurentia (Laurussia) in the south tropical latitude (Fig. 1B). The Llandovery is characterized by a high runoff (Fig. 3A) and hence weathering, and CO_2 is still maintained at low levels (8 to 9 PAL). But the drastic decrease of the discharge of the continental water induces low weathering rates and thus very high $p\text{CO}_{2\text{atm}}$ levels (22 PAL) in the Early Devonian. The main culprit for this CO_2 rise is the strong decrease in global runoff triggered by the tectonic drift (Table 1). First there are no more continental landmasses around 10  N (Fig. 3C), where the model should predict a peak in runoff (Fig. 3B). Second, the assemblage of Baltica and Laurentia south of the paleoequator enhanced the continentality effect, inducing a reduction of the runoff in the 10  S zone.

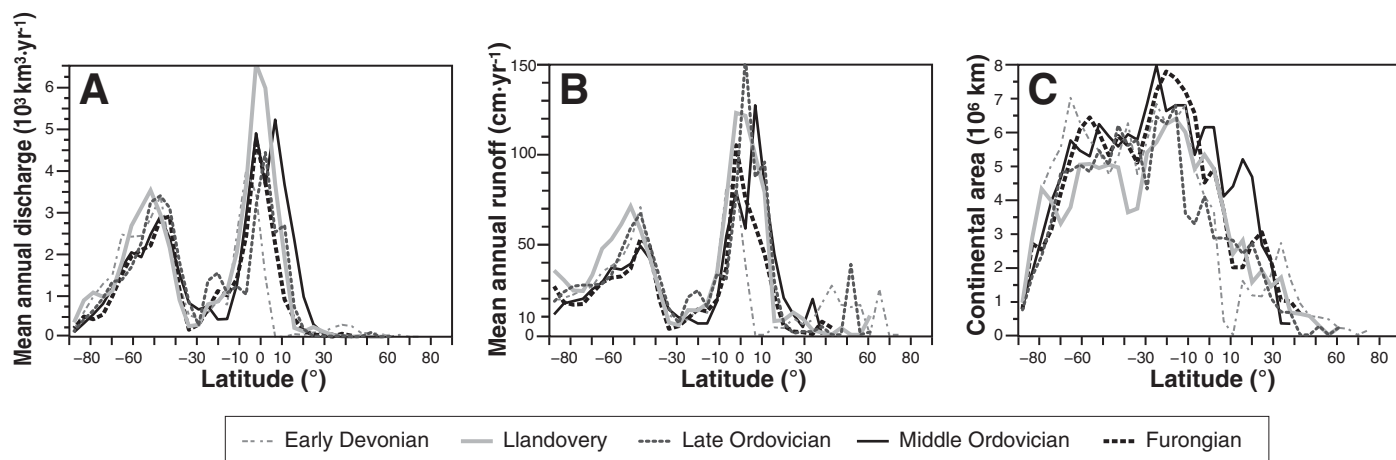


Figure 3. (A) Mean annual continental fluvial discharge to the ocean (*NormSr* run). (B) Mean annual runoff (*NormSr* run). (C) Continental surface. Atmospheric $p\text{CO}_2$ fixed at 15 (preindustrial atmospheric level [PAL], 4200 ppmv) in all simulations.

Continental Temperatures

Figure 4 displays the evolution of the mean annual continental surface temperatures through the early Paleozoic, as simulated by GEOCLIM. The most obvious result is the onset of a cold climate window between the Middle Ordovician and the Llandovery. Starting with high values in the Furongian (~16 °C; Table 1), the continental temperatures remain low from the Middle Ordovician to the Llandovery (~13.5 °C). Then simulated continental temperatures rise again in the Early Devonian to values around 16 °C. The *Ref* simulations results show a similar trend with lower temperatures in the Cambrian–Early Ordovician and higher ones for the rest of the studied interval (Fig. 4A). This suggests a major impact of the paleogeographic changes and a strong influence of the continental rock

weathering especially during the Late Ordovician–Llandovery interval. The coupled climate-carbon model thus predicts the onset of a cool time window linked to the weathering of fresh volcanic rocks and to the movement of the continents through the climatic zones. It is worth mentioning that, despite the motion of large continental blocks across the ITCZ from the Early Ordovician to the Llandovery, enhanced continental weathering forces the continents to cool through enhanced CO_2 consumption. Similarly a warming of about 3.8 °C due to the paleogeographic changes has been suggested for the Cretaceous period (Donnadieu et al., 2006a).

Another way to validate our CO_2 estimates is to compare individual climate changes simulated with GEOCLIM to independent estimates of changes through the time interval. Our modeled continental temperature drawdown trend during the Ordovician–Silurian is relatively congruent

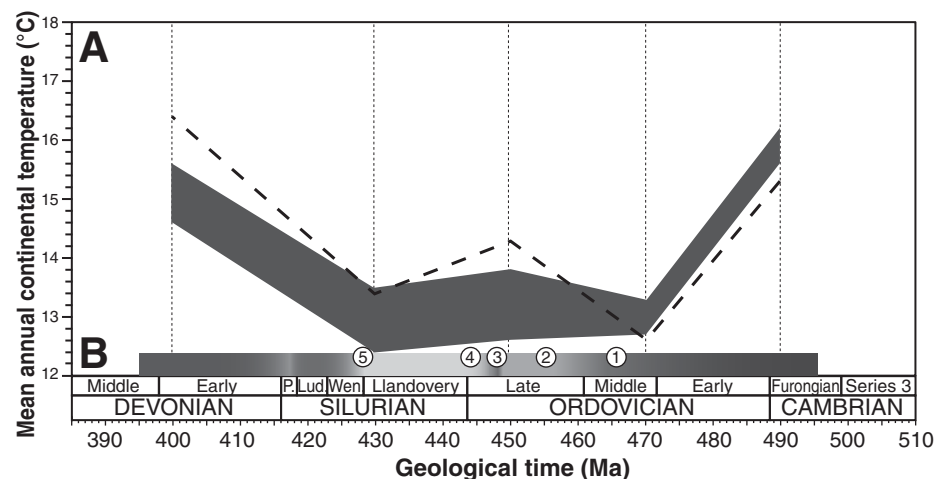


Figure 4. (A) Calculated mean continental temperatures in the early Paleozoic. The gray curve stands for the results of both the *NormSr* and *HighSr* simulations, in which siliciclastic rock outcrops percentage per grid cells change through time. The dashed line stands for the results of the *Ref* simulation, in which volcanic rock outcrops percentage per cell is fixed at their present-day value (11%, Dürr et al., 2005). (B) Climatic trend reconstructed from the interpretation of geological record or reconstructed proxies: ① initiation of the cooling trend (early Middle Ordovician; Trotter et al., 2008); ② Guttenberg $\delta^{13}\text{C}$ excursion (GICE) peak

often interpreted as the first glacial event (*caudatus* conodont zone, early Katian; Armstrong et al., 2009; Ainsaar et al., 2010; Buggisch et al., 2010); ③ occurrence of the short, warmer Boda Event (*rugatus* conodont zone, late Katian; Armstrong et al., 2009; Fortey and Cocks, 2005); ④ Hirnantian glacial maximum (Ghienne et al., 2003; Le Heron et al., 2007); ⑤ possible end of the glacial interval (late Telychian), shown by the latest geological glacial records in South America (Díaz-Martínez et al., 1997; Schönién et al., 1999; Cramer and Saltzman, 2007; Lehnert et al., 2010). Between ② and ⑤, the sedimentologic record clearly indicates the presence of continental ice sheet on Gondwana (North Africa, South America, and South Europe; Díaz-Martínez and Grahn, 1997; Ghienne et al., 2010; Gutiérrez-Marco et al., 2010; Lehnert et al., 2010; Videt et al., 2010). Dark gray corresponds to colder periods; light gray to white correspond to cooler periods. P.—Pridoli; Lud—Ludlow; Wen—Wenlock.

with the climatic trend interpreted from the sedimentologic record and the isotopic proxies (Fig. 4B). The cooling interval may have started in the Early Ordovician (Fig. 4B ①; Trotter et al., 2008), followed by a glacial period ranging from middle Upper Ordovician to the late Llandovery (Fig. 4B ②–⑤) and including the Hirnantian glacial maximum (Fig. 4B ④; Ghienne et al., 2003, 2010; Le Heron et al., 2007; Le Heron and Dowdeswell, 2009). This glacial period is characterized by several worldwide, recorded, positive $\delta^{13}\text{C}$ excursions and by Gondwanan sedimentologic features showing the presence of a continental ice sheet and the effects of glacio-eustatic processes (e.g., diamictites, tillites, and paleovalleys) (Díaz-Martínez et al., 1997; Ghienne et al., 2010; Gutiérrez-Marco et al., 2010; Lehnert et al., 2010; Videt et al., 2010). This glacial interval probably began with the worldwide positive Guttenberg $\delta^{13}\text{C}$ excursion (GICE event) in the middle Katian (Fig. 4B ②), interpreted as an enhanced burial of organic matter in poorly oxygenated water masses during a shift in the style of platform sedimentation from tropical-type to temperate-type carbonates (Ainsaar et al., 1999, 2010; Pancost et al., 1999; Pope and Steffen, 2003; Saltzman and Young, 2005; Armstrong et al., 2009; Buggisch et al., 2010).

The glacial interval ended during the latest Llandovery (Fig. 4B ⑤) with the last diamictites recorded in western Gondwana (e.g., Bolivia and Peru; Schönián et al., 1999; Cramer and Saltzman, 2007; Díaz-Martínez and Grahn, 2007). The existence of such a cool time window is also sustained by independent studies of the pelagic fauna distribution during the Late Ordovician (see Vandenbroucke et al., 2010).

We cannot predict the potential ice-sheet geographical extension corresponding to our simulated climate because the FOAM GCM is not coupled to an ice-sheet model in this study. Nevertheless, previous modeling studies using GCM asynchronously coupled to an ice-sheet model have shown that the $p\text{CO}_{2\text{atm}}$ must have fallen below 15 PAL (with a low sea level and reduced poleward, ocean-heat transport) for the lower Late Ordovician and below 10 PAL (using constant orbital parameters) or even 8 PAL (using time-varying orbital parameters) for the upper Late Ordovician in order to initiate the growth of permanent ice sheets during the Late Ordovician (Herrmann et al., 2004a, 2004b). Those studies also calculated continental temperatures between 13 and 15.5 °C. Our modeled $p\text{CO}_{2\text{atm}}$ and continental temperature values, especially with the *HighSr* simulations, for the Middle Ordovician and the Llandovery (Table 1) are very close to the thresholds as determined by Herrmann et al. (2004a, 2004b) and may potentially allow the presence of perennial snow cover or ice sheet on continents, which could be consistent with the sedimentologic record.

Surface-Seawater Temperatures

The most recent estimations of the seawater temperatures during the early Paleozoic are based on apatite $\delta^{18}\text{O}$ measurements (Wenzel et al., 2000; Bassett et al., 2007; Trotter et al., 2008; Buggisch et al., 2010). Because the climate module of GEOCLIM is a GCM, calculated temperatures at the sites sampled by these published studies can be compared to the reconstructed temperatures. Given the low spatial resolution of the FOAM GCM (7.5° longitude \times 4.5° latitude), the information available in the publications for the sampling sites, and the uncertainty inherent to the accuracy and the age of the paleogeographic reconstruction used in the study, 25 sites were located on the model grid map (Fig. 5A). The surface-seawater temperatures calculated with GEOCLIM at these locations are then compared to the reconstructed temperatures (Fig. 5B).

From the Middle Ordovician to the early Wenlock, calculated temperatures fit quite well the range of the reconstructed geological proxies. By contrast, the temperatures modeled for the Early Ordovician and the

first part of the Middle Ordovician are markedly lower than the temperatures inferred from biogenic apatite $\delta^{18}\text{O}$. As a result, the model misses the large temperature decrease highlighted by conodont apatite $\delta^{18}\text{O}$ from the Furongian to the Middle Ordovician. Importantly, the model is unable to produce a surface-seawater temperature of ~42 °C as reconstructed by Bassett et al. (2007) from the Lange Ranch section (central Texas, USA; point Ba1, Fig. 5A) and by Trotter et al. (2008) from the Georgina Basin (Queensland, Australia) (samples GB90-003/02/03-04 in Trotter et al., 2008; point T1, Fig. 5A). Because these very high temperatures and the increasing $\delta^{18}\text{O}$ trend are observed in both Australian and American samples (Bassett et al., 2007; Trotter et al., 2008), it seems unlikely that they result from diagenetic processes. It could be noted that GEOCLIM has been run as a slab ocean model, which tends to induce a narrow ITCZ, and therefore the temperatures simulated near the border of the ITCZ may not be as reliable as the temperatures from other parts of the oceans. However, because the temperatures simulated for the locations near the ITCZ during the Late Ordovician and the Llandovery are in good agreement with apatite $\delta^{18}\text{O}$, we do not think that the discrepancies observed in the Early Ordovician between the isotopic and modeled temperatures are due to the model configuration only (see discussion below). In addition, the simulated temperature of the air at the surface of the ocean, which may be closer to the temperature of a thin and localized water mass, is ~34 °C, 4 °C above the calculated seawater temperature at the point T1, but still below the temperature ~42 °C inferred from apatite $\delta^{18}\text{O}$ measurements.

A temperature of ~42 °C is at the upper limit of the modern surface-seawater temperature range in small and closed seas (e.g., Red Sea and Sunda Sea), and is not easily reached in open seas. In addition, an extrapolation of the results of our GCM simulations suggests that a temperature about 42 °C with GEOCLIM requires a $p\text{CO}_{2\text{atm}}$ as high as 125 PAL. Such high $\text{CO}_{2\text{atm}}$ contents would result in temperatures as high as 50 °C at some locations in the tropical ocean (on the northwest coast of Laurentia, east coast of Antarctica, and west coast of Australia). Such high temperatures might be lethal for many organisms (Ross, 1995). Nevertheless, these temperatures higher than 40 °C were calculated assuming seawater $\delta^{18}\text{O}$ of -1‰ for an ice-free ocean. If the required CO_2 (125 PAL) is too high, then we are once again left with the question of the actual value of the seawater $\delta^{18}\text{O}$ at the beginning of the Phanerozoic. Models of the geological water cycle have been able to reproduce large variations in seawater $\delta^{18}\text{O}$, down to values of -4‰ or -6‰ in the Cambrian or lowermost Ordovician depending on the value of low-temperature alteration (Veizer et al., 1997; Wallmann et al., 2001b; Jaffrés et al., 2007). Calculated temperatures from conodont apatite $\delta^{18}\text{O}$ would drop down to 29 °C or even 20 °C in the lowermost Ordovician, if a value of -4‰ or -6‰ was assumed for seawater $\delta^{18}\text{O}$, respectively. This implies that our simulations could be reconciled with available isotopic data, if an increase in seawater $\delta^{18}\text{O}$ occurred from the lowermost to the Middle Ordovician, partly contributing to the recorded increase in apatite $\delta^{18}\text{O}$ values during this period.

UNCERTAINTIES AND LIMITATIONS

Modeling climate and global geochemical cycles during the early Paleozoic involves numerous processes, which are sometimes difficult to constrain.

(1) The solid Earth CO_2 degassing was kept constant at its present-day level because there is no consensus about the Earth degassing in the distant past. Assessing the Earth degassing at a large scale during the Paleozoic is probably uncertain and inaccurate regarding the high variability of the present-day volcanic CO_2 emissions and the impossibility to constrain the Paleozoic submarine volcanoes activity, the deep-sea carbonate deposition and recycling at subduction zones, and the seafloor spreading rates (see

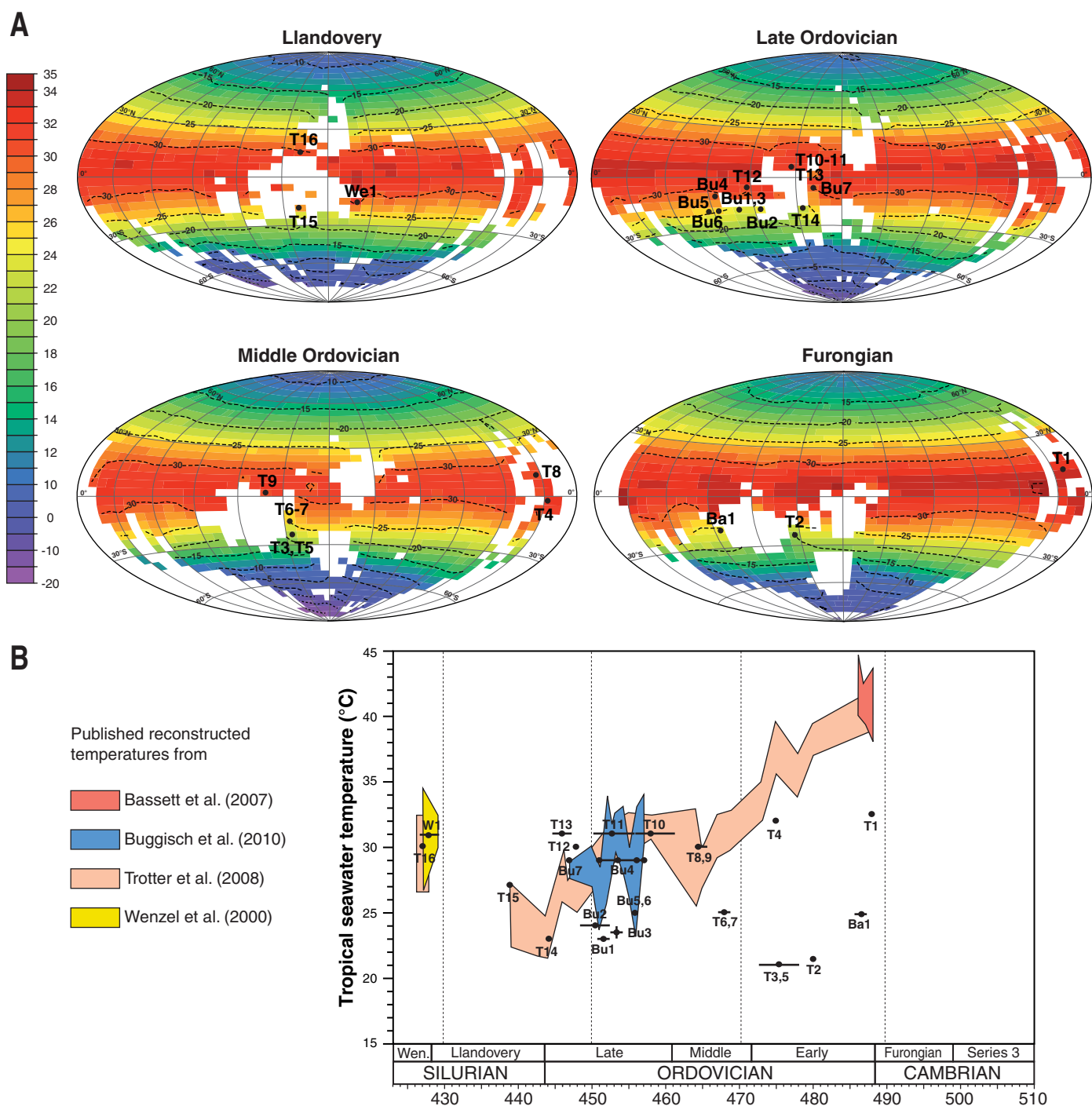


Figure 5. (A) Modeled latitudinal distribution of the mean annual temperatures, with the location of the 25 sampling sites yielding published estimated temperatures based on apatite $\delta^{18}\text{O}$ measurements (Ba—Bassett et al., 2007; Bu—Buggisch et al., 2010; T—Trotter et al., 2008; W—Wenzel et al., 2000) for the first four simulated time slices. (B) Modeled temperatures (black points) calculated with the *NormSr* configuration at the 25 sampling points, used for comparison with the published reconstructed temperatures (cf. references above). We assigned the age of each formation to the model output. Temperatures from conodont $\delta^{18}\text{O}$ have been calculated as in Trotter et al. (2008), using the equation of Kolodny et al. (1983) and assuming a $\delta^{18}\text{O}$ of seawater of -1‰ Vienna standard mean ocean water (VSMOW) with no adjustment for ice-volume effects. Temperatures of Bassett et al. (2007) and of Buggisch et al. (2010) are based on $\delta^{18}\text{O}$ values normalized to NBS (National Institute of Standards and Technology) $120\text{c} = 21.7\text{‰}$ VSMOW. Wen—Wenlock.

Kerrick, 2000, for a detailed discussion). Recent estimations of the sea-floor spreading rate for the past 200 million years contradict the generally accepted long-term decrease in spreading rates since the Cretaceous (as predicted by Gaffin, 1987). Conversely, they suggest a relatively constant spreading rate over the past 200 million years (Rowley, 2002) or even an increase (Cogné and Humler, 2004). Given these uncertainties even for recent periods, adopting a constant degassing rate in the Paleozoic might be a rather conservative hypothesis. It cannot be ruled out that it was not the case given the absence of accurate reconstructions. Nevertheless, even if we account for the sole reconstruction of the degassing rate for the Paleozoic (Gaffin, 1987), it suggests a roughly constant flux in the 500–400 Ma time interval. As a result, the calculated absolute $p\text{CO}_{2\text{atm}}$ values would shift, but the trend through time would be similar.

(2) The exact surface of the continental shelves and the exact localization of the topographic barriers and arcs could also be doubtful for the lesser known regions. However, many sedimentologic and tectonic studies now allow realistic reconstruction of the general shorelines and of the location of the terranes, with a sufficient precision for the grid of GEOCLIM (see Blakey, 2007; Cocks and Torsvik, 2002, and the references therein).

(3) As most of the early Paleozoic rocks are partially to totally eroded, the extent and geographic location of the volcanic and shield rocks has not been spatially constrained in this study. The fixed fraction of outcropping silicate rocks for all continental grid elements could result in an underestimation of the impact of the volcanic rock weathering on the CO_2 consumption, if those rocks would be preferentially located in the ITCZ.

Moreover, the FOAM GCM has been used in a slab mixed-layer mode. A slab ocean model lacks the dynamic feedback of the ocean on climate (Poulsen et al., 2001). The use of the slab ocean model commonly induces a slight extension of the subsiding regions; therefore the equator belt tends to be narrower than with a full dynamic ocean model. To explore the impact of accounting for the ocean dynamics on our results, a sensitivity test for the Furongian geography has been run with FOAM in its fully dynamic version. Results are similar compared to the slab simulation output, with differences less than 0.5 °C for the modeled continental temperatures, and less than 4 $\text{cm}\cdot\text{yr}^{-1}$ for the continental runoff. This could suggest that our results computed with the slab-ocean FOAM remain correct at the first order.

CONCLUSIONS

In the present contribution, we use the coupled climate-carbon model GEOCLIM to explore the long-term climatic trend of the early Paleozoic. Two forcing factors were tested: the paleogeographic changes and the weathering of siliciclastic rocks, especially of the fresh volcanic rocks. The proportions of outcropping volcanic rocks doubled between the Furongian and the Late Ordovician, and then slightly decreased during the Llandovery with both *NormSr* and *HighSr* simulations. The importance of volcanic rock weathering in the $\text{CO}_{2\text{atm}}$ budget fluctuates through the early Paleozoic but reaches its maximum level in the Late Ordovician.

Our simulations show a U-shaped $\text{CO}_{2\text{atm}}$ curve with a low $\text{CO}_{2\text{atm}}$ time window from the Middle Ordovician to the Llandovery. The Furongian dropdown of the $\text{CO}_{2\text{atm}}$ forces the mean continental temperatures to decrease by about 3 °C. These calculated cooler climatic conditions persist until the Llandovery, and thus possibly facilitate the onset of glacial pulses during the Late Ordovician–Llandovery time. Modeled mean continental temperature for the Early Devonian is 16 °C.

The low $\text{CO}_{2\text{atm}}$ window is due to the combined effect of the northward drift of the paleocontinents across the ITCZ and the increase in the weathering of fresh volcanic rocks. The enhanced weathering of volcanic rocks is responsible for about 33% of the CO_2 decrease in the Late Ordovician,

the rest being related to the plate motion through the ITCZ and induced continental climate changes, which promote CO_2 consumption by weathering. Further investigations should focus on the reconstruction of the $^{87}\text{Sr}/^{86}\text{Sr}$ ratio of the Middle Ordovician–Llandovery volcanic rocks and on the role of second-order changes in paleogeography to determine more precisely their impact on the $\text{CO}_{2\text{atm}}$ and climate of the early Paleozoic.

ACKNOWLEDGMENTS

This work was financed by the National Agency for Research (CNRS). It is a contribution to the ANR ACCRO-Earth (no. ANR-06-BLAN-0347) and the ANR COLORS (no. ANR-09-JCJC-0105). We acknowledge the Associate Editor and the two anonymous reviewers for their constructive comments that have helped to improve this manuscript. We thank the participants of the project SYSTER “*Le climat de l’Ordovicien: Modèles et données*” for their beneficial discussions.

REFERENCES CITED

- Ainsaar, L., Meidla, T., and Martma, T., 1999, Evidence for a widespread carbon isotopic event associated with late Middle Ordovician sedimentological and faunal changes in Estonia: *Geological Magazine*, v. 136, p. 49–62.
- Ainsaar, L., Kaljo, D., Martma, T., Meidla, T., Männik, P., and Nõlvak, J., 2010, Middle and Upper Ordovician carbon isotope chemostratigraphy in Baltoscandia: A correlation standard and clues to environmental history: *Palaeogeography, Palaeoclimatology, Palaeoecology*, v. 294, p. 189–201.
- Armstrong, H.A., Abbott, G.D., Turner, B.R., Makhlof, I.M., Muhammad, A.B., Pedenchouk, N., and Peters, H., 2009, Black shale deposition in an Upper Ordovician–Silurian permanently stratified, peri-glacial basin, southern Jordan: *Palaeogeography, Palaeoclimatology, Palaeoecology*, v. 273, p. 368–377.
- Bao, H.M., Lyons, J.R., and Zhou, C., 2008, Triple oxygen isotope evidence for elevated CO_2 levels after a Neoproterozoic glaciation: *Nature*, v. 453, p. 504–506.
- Bassett, D., MacLeod, K.G., Miller, J.F., and Ethington, R.L., 2007, Oxygen isotopic composition of biogenic phosphate and the temperature of the Early Ordovician seawater: *Palaos*, v. 22, p. 98–103.
- Berner, R.A., 1991, A model for atmospheric CO_2 over Phanerozoic time: *American Journal of Sciences*, v. 291, p. 339–376.
- Berner, R.A., 1998, The carbon cycle and CO_2 over Phanerozoic time: The role of land plants: *London, Philosophical Transactions of the Royal Society*, v. 353, p. 75–82.
- Berner, R.A., 2004, *The Phanerozoic Carbon Cycle: CO_2 and O_2* : Oxford University Press, 150 p.
- Berner, R.A., 2006a, GEOCARBSULF: A combined model for Phanerozoic atmospheric O_2 and CO_2 : *Geochimica et Cosmochimica Acta*, v. 70, p. 5633–5664.
- Berner, R.A., 2006b, Inclusion of the weathering of volcanic rocks in the GEOCARBSULF model: *American Journal of Science*, v. 306, p. 295–302.
- Berner, R.A., 2008, Addendum to “inclusion of the weathering of volcanic rocks in the GEOCARBSULF model”: *American Journal of Science*, v. 308, p. 100–103.
- Berner, R.A., and Kothavala, Z., 2001, GEOCARB III: A revised model of atmospheric CO_2 over Phanerozoic time: *American Journal of Sciences*, v. 301, p. 182–204.
- Blakey, R.C., 2007, Carboniferous–Permian paleogeography of the assembly of Pangea, in Wong, T.E., ed., *Fifteenth International Congress on Carboniferous and Permian Stratigraphy*: Utrecht, the Netherlands, Royal Netherlands Academy of Arts and Sciences, p. 443–465.
- Boucot, A.J., and Gray, J., 2001, A critique of Phanerozoic climatic models involving changes in the CO_2 content of the atmosphere: *Earth-Science Review*, v. 56, p. 1–159.
- Boucot, A.J., Xu, C., and Scotese, C.R., 2004, Phanerozoic climatic zones and paleogeography with a consideration of atmospheric CO_2 level: *Paleontological Journal*, v. 38, p. 115–122.
- Buggisch, W., Joachimski, M.M., Lehnert, O., Bergström, S., Repetski, J.E., and Webers, G.F., 2010, Did intense volcanism trigger the first Late Ordovician icehouse?: *Geology*, v. 38, p. 327–330.
- Campos Neto, M.C., and Figueiredo, C.H., 1995, The Rio Doce orogeny, southeastern Brazil: *Journal of South American Earth Sciences*, v. 8, p. 143–162.
- Cocks, L.R.M., and Torsvik, T.H., 2002, Earth geography from 500 to 400 million years ago: A faunal and palaeomagnetic review: *Journal of the Geological Society of London*, v. 159, p. 631–644.
- Cogné, J.P., and Humler, E., 2004, Temporal variation of oceanic spreading and crustal production rates during the last 180 My: *Earth and Planetary Science Letters*, v. 227, p. 427–439.
- Cramer, B.D., and Saltzman, M.R., 2007, Fluctuations in epeiric sea carbonate production during Silurian positive carbon isotope excursions: A review of proposed paleoceanographic models: *Palaeogeography, Palaeoclimatology, Palaeoecology*, v. 245, p. 37–45.
- Crowley, T.J., and Baum, S.K., 1995, Reconciling Late Ordovician (440 Ma) glaciation with very high ($14\times$) CO_2 levels: *Journal of Geophysical Research*, v. 100, p. 1093–1101.
- Crowley, T.J., Baum, S.K., and Hyde, W.T., 1991, Climate model comparison of Gondwanan and Laurentide glaciations: *Journal of Geophysical Research*, v. 96, no. 5, p. 9217–9226.
- Demoux, A., Kröner, A., Hegner, E., and Badarch, G., 2009, Devonian arc-related magmatism in the Tsel terrane of SW Mongolia: Chronological and geochemical evidence: *Journal of the Geological Society of London*, v. 166, no. 3, p. 459–471.

- Dessert, C., Dupré, B., François, L.M., Schott, J., Gaillardet, J., Chakrapani, G., and Bajpai, S., 2001, Erosion of Deccan Traps determined by river geochemistry: Impact on the global climate and the $^{87}\text{Sr}/^{86}\text{Sr}$ ratio of seawater: *Earth and Planetary Science Letters*, v. 188, no. 3–4, p. 459–474.
- Dessert, C., Dupré, B., Gaillardet, J., François, L.M., and Allègre, C.J., 2003, Basalt weathering laws and the impact of basalt weathering on the global carbon cycle: *Chemical Geology*, v. 202, p. 257–273.
- Dewey, J.F., 2005, Orogeny can be very short: *Proceedings of the National Academy of Sciences*, v. 43, p. 1–8.
- Díaz-Martínez, E., and Grahn, Y., 2007, Early Silurian glaciation along the western margin of Gondwana (Peru, Bolivia, and northern Argentina): Palaeogeographic and geodynamic setting: *Palaeogeography, Palaeoclimatology, Palaeoecology*, v. 245, p. 62–81.
- Donnadieu, Y., Goddérís, Y., Ramstein, G., Nédélec, A., and Meert, J., 2004, A “snowball Earth” climate triggered by continental breakup through changes in runoff: *Letters to Nature*, v. 428, p. 303–306.
- Donnadieu, Y., Pierrehumbert, R., Jacob, R., and Fluteau, F., 2006a, Modelling the primary control of paleogeography on Cretaceous climate: *Earth and Planetary Science Letters*, v. 248, p. 426–437.
- Donnadieu, Y., Goddérís, Y., Pierrehumbert, R. T., Dromart, G., Fluteau, F., and Jacob, R., 2006b, A GEOCLIM simulation of climatic and biogeochemical consequences of Pangea breakup: *Geochemistry, Geophysics, Geosystems*, v. 7, 21 p., doi: 10.1029/2006GC001278.
- Dupré, B., Dessert, C., Oliva, P., Goddérís, Y., Viers, J., François, L.M., Millot, R., and Gaillardet, J., 2003, River, chemical weathering, and Earth’s climate: *Comptes Rendus Geoscience*, v. 335, no. 16, p. 1141–1160.
- Dürr, H.H., Meybeck, M., and Dürr, S.H., 2005, Lithologic composition of the Earth’s continental surfaces derived from a new digital map emphasizing riverine material transfer: *Global Biogeochemical Cycles*, v. 19, 22 p., doi: 10.1029/2005GB002515.
- Francis, E.H., 1988, Mid-Devonian–Permian activity in the Caledonian–Appalachian orogen: *The Geological Society of London, Special Publication*, v. 38, p. 573–584.
- Fortey, R.A., and Cocks, L.R.M., 2005, Late Ordovician global warming—The Boda event: *Geology*, v. 33, p. 405–408.
- Gaffin, S., 1987, Ridge volume dependence on seafloor generation rate and inversion using long term sea-level change: *American Journal of Science*, v. 287, p. 596–611.
- Gaillardet, J., Dupré, B., Louvat, P., and Allègre, C.J., 1999, Global silicate weathering and CO_2 consumption rates deduced from the chemistry of the large rivers: *Chemical Geology*, v. 159, p. 3–30.
- Galy, A., France-Lanord, C., and Derry, L.A., 1999, The strontium budget of Himalayan rivers in Nepal and Bangladesh: *Geochimica et Cosmochimica Acta*, v. 63, p. 1905–1925.
- Ganis, G.R., and Wise, D.U., 2008, Taconic events in Pennsylvania: Datable phases of a ~20 m.y. orogeny: *American Journal of Science*, v. 308, p. 167–183.
- Ghienne, J.F., 2003, Late Ordovician sedimentary environments, glacial cycles, and post-glacial transgression in the Taoudeni Basin, West Africa: *Palaeogeography, Palaeoclimatology, Palaeoecology*, v. 189, p. 117–145.
- Ghienne, J.F., Monod, O., Kozlu, H., and Dean, W.T., 2010, Cambrian–Ordovician depositional sequences in the Middle East: A perspective from Turkey: *Earth-Science Reviews*, v. 101, p. 101–145.
- Gibbs, M.T., Barron, E.J., and Kump, L.R., 1997, An atmospheric pCO_2 threshold for glaciation in the Late Ordovician: *Geology*, v. 25, p. 447–450.
- Goddérís, Y., and François, L.M., 1995, The Cenozoic evolution of the strontium and carbon cycles: Relative importance of continental erosion and mantle exchanges: *Chemical Geology*, v. 126, 169–190.
- Goddérís, Y., and Joachimski, M.M., 2004, Global change in the Late Devonian: Modelling the Frasnian–Famennian short-term carbon isotope excursions: *Palaeogeography, Palaeoclimatology, Palaeoecology*, v. 202, p. 309–329.
- Goddérís, Y., Nédélec, A., Donnadieu, Y., Dupré, B., Dessert, C., François, L.M., Grard, A., and Ramstein, G., 2003, The Sturtian glaciation: Fire and ice: *Earth and Planetary Science Letters*, v. 211, p. 1–12.
- Goddérís, Y., Donnadieu, Y., De Vargas, C., Pierrehumbert, R.T., Dromart, G., and van de Schootbrugge, B., 2008, Causal of causal link between the rise of nanoplankton calcification and a tectonically driven massive decrease in the Late Triassic atmospheric CO_2 : *Earth and Planetary Science Letters*, v. 267, p. 247–255.
- Gough, D. O., 1981, Solar interior structure and luminosity variations: *Solar Physics*, v. 74, p. 21–34.
- Gradstein, F.M., Ogg, J.G., Smith, A.G., Agterberg, F.P., Bleeker, W., Cooper, R.A., Davydov, V., Gibbard, P., Hinnov, L.A., House, M.R., Lourens, L., Luterbacher, H.P., McArthur, J., Melchin, M.J., Robb, L.J., Shergold, J., Villeneuve, M., Wardlaw, B.R., Ali, J., Brinkhuis, H., Hilgen, F.J., Hooker, J., Howarth, R.J., Knoll, A.H., Laskar, J., Monechi, S., Plumb, K.A., Powell, J., Raffi, I., Röhl, U., Sadler, P., Sanfilippo, A., Schmitz, B., Shackleton, N.J., Shields, G.A., Strauss, H., Van Dam, J., van Kolfshoten, T., Veizer, J., and Wilson, D., 2004, *A Geologic Time Scale*: Cambridge University Press, 589 p.
- Gutiérrez-Marco, J.C., Ghienne, J.F., Bernárdez, E., and Hacer, M.P., 2010, Did the Late Ordovician African ice sheet reach Europe? *Geology*, v. 38, p. 279–282.
- Haq, B.U., and Schutter, S.R., 2008, A chronology of Paleozoic sea-level changes: *Science*, v. 322, p. 64–69.
- Herrmann, A.D., Patzkowsky, M.E., and Pollard, D., 2004a, The impact of paleogeography, pCO_2 , poleward ocean heat transport, and sea level change on global cooling during the Late Ordovician: *Palaeogeography, Palaeoclimatology, Palaeoecology*, v. 206, p. 59–74.
- Herrmann, A.D., Haupt, B.J., Patzkowsky, M.E., Seidov, D., and Slingerland, R.L., 2004b, Response of Late Ordovician paleoceanography to changes in sea level, continental drift, and atmospheric pCO_2 : Potential causes for long-term cooling glaciation: *Palaeogeography, Palaeoclimatology, Palaeoecology*, v. 210, p. 385–401.
- Hibbard, J.P., Stoddard, E.F., Secor, D.T., and Dennis, A.J., 2002, The Carolina Zone: Overview of Neoproterozoic to early Paleozoic peri-Gondwanan terranes along the eastern flank of the southern Appalachians: *Earth-Science Reviews*, v. 57, p. 299–339.
- Huff, W.D., 2008, Ordovician K-bentonites: Issues in interpreting and correlating ancient tephros: *Quaternary International*, v. 178, p. 276–187.
- Jacob, R., 1997, Low frequency variability in a simulated atmosphere ocean system [Ph.D. thesis]: University of Wisconsin–Madison, 170 p.
- Jaffrés, J.B.D., Shields, G.A., and Wallmann, K., 2007, The oxygen isotope evolution of seawater: A critical review of a long-standing controversy and an improved geological water cycle model for the past 3.4 billion years: *Earth-Science Reviews*, v. 83, p. 83–122.
- Kerrick, D.M., 2000, Present and past nonanthropogenic CO_2 degassing from the solid Earth: *Reviews of Geophysics*, v. 39, no. 4, p. 565–585.
- Kolodny, Y., Luz, B., and Navon, O., 1983, Oxygen isotope variations in phosphate of biogenic apatites, I. Fish bone apatite—Rechecking the rules of the game: *Earth and Planetary Science Letters*, v. 64, p. 398–404.
- Kump, L.R., and Arthur, M.A., 1997, Global chemical erosion during the Cenozoic: Weatherability balances the budget, in: Ruddiman, W.F., ed., *Tectonic and Climate Change*: New York, Plenum Press, p. 399–426.
- Kump, L.R., Arthur, M.A., Patzkowsky, M.E., Gibbs, M.T., Pinkus, D.S., and Sheehan, P.M., 1999, A weathering hypothesis for glaciation at high atmospheric pCO_2 during the Late Ordovician: *Palaeogeography, Palaeoclimatology, Palaeoecology*, v. 152, p. 173–187.
- Kump, L.R., Brantley, S.L., and Arthur, M.A., 2000, Chemical weathering, atmospheric CO_2 , and climate: *Annual Review of Earth and Planetary Sciences*, v. 28, p. 611–667.
- Lefebvre, B., Servais, T., François, L., and Averbuch, O., 2010, Did a Katian large igneous province trigger the Late Ordovician glaciation?: A hypothesis tested with a carbon cycle model: *Palaeogeography, Palaeoclimatology, Palaeoecology*, v. 296, no. 3–4, p. 309–319.
- Le Heron, D., and Dowdeswell, J.A., 2009, Calculating ice volumes and ice flux to constrain the dimensions of a 440 Ma North African ice sheet: *Journal of the Geological Society of London*, v. 166, p. 277–281.
- Le Heron, D.P., Ghienne, J.-F., El Houicha, M., Khoukhi, Y., and Rubino, J.-L., 2007, Maximum extent of ice sheets in Morocco during the Late Ordovician glaciation: *Palaeogeography, Palaeoclimatology, Palaeoecology*, v. 245, p. 200–226.
- Lehnert, O., Männik, P., Joachimski, M.M., Calner, M., and Frýda, J., 2010, Paleoclimate perturbations before the Scheinwoodian glaciation: A trigger for extinctions during the “Ireviken Event”: *Palaeogeography, Palaeoclimatology, Palaeoecology*, v. 296, no. 3–4, p. 320–331.
- McKerrow, W.S., and Scotese, C.R., eds., 1990, *Paleozoic Paleogeography and Biogeography*: The Geological Society of London Memoir 12, p. 1–435.
- Min, K., Renne, P.R., and Huff, W.D., 2001, $^{40}\text{Ar}/^{39}\text{Ar}$ dating of Ordovician K-bentonites in Laurentia and Baltoscandia: *Earth and Planetary Science Letters*, v. 185, p. 121–134.
- Oliva, P., Viers, J., and Dupré, B., 2003, Chemical weathering in granitic crystalline environments: *Chemical Geology*, v. 202, p. 225–256.
- Pancost, R.D., Freeman, K.H., and Patzkowsky, M.E., 1999, Organic-matter source variation and the expression of a late Middle Ordovician carbon isotope excursion: *Geology*, v. 27, no. 11, p. 1015–1018.
- Papanastassiou, D.A., and Wasserburg, G.J., 1969, Initial strontium isotopic abundances and the resolution of small time differences in the formation of planetary objects: *Earth and Planetary Science Letters*, v. 5, p. 361–376.
- Patzkowsky, M.E., Slupik, L.M., Arthur, M.A., Pancost, R.D., and Freeman, K.H., 1997, Late Middle Ordovician environmental change and extinction: Harbinger of the Late Ordovician or continuation of Cambrian patterns? *Geology*, v. 25, p. 911–914.
- Pope, M.C., and Steffen, J.B., 2003, Widespread, prolonged late Middle to Late Ordovician upwelling in North America: A proxy record of glaciation? *Geology*, v. 31, no. 1, p. 63–66.
- Poulsen, C.J., Barron, E.J., Arthur, M.A., and Peterson, W.H., 2001, Response of the mid-Cretaceous global oceanic circulation to tectonic and CO_2 forcing: *Paleoceanography*, v. 16, no. 6, p. 576–592.
- Poussart, P.F., Weaver, A.J., and Barnes, C.R., 1999, Late Ordovician glaciation under high atmospheric CO_2 : A coupled model analysis: *Paleoceanography*, v. 14, p. 542–558.
- Ross, D.A., 1995, *Introduction to Oceanography*: New York, Harper Collins College Publishers.
- Rowley, D.B., 2002, Rate of plate creation and destruction: 180 Ma to present: *Geological Society of America Bulletin*, v. 114, p. 927–933.
- Royer, D.L., 2006, CO_2 -forced climate thresholds during the Phanerozoic: *Geochimica et Cosmochimica Acta*, v. 70, p. 5665–5675.
- Saltzman, M.R., and Young, S.A., 2005, Long-lived glaciation in the Late Ordovician?: Isotopic and sequence-stratigraphic evidence from western Laurentia: *Geology*, v. 33, no. 2, p. 109–112.
- Samson, S.D., 1996, $^{40}\text{Ar}/^{39}\text{Ar}$ and Nd–Sr isotopic characteristics of mid-Ordovician North American K-bentonites: A test of early Paleozoic Laurentia–Gondwana interactions: *Tectonics*, v. 15, p. 1084–1092.
- Schönian, F., Egenhoff, S., Marcinek, J., and Erdtmann, B.-D., 1999, Glaciation at the Ordovician–Silurian boundary in southern Bolivia: *Acta Universitatis Carolinae Geologica*, v. 43, p. 175–178.
- Scotese, C.R., 2004, A continental drift flipbook: *The Journal of Geology*, v. 112, p. 729–741.
- Stampfli, G.M., and Borel, G.D., 2002, A plate tectonic model for the Paleozoic and Mesozoic constrained by dynamic plate boundaries and restored synthetic oceanic isochrones: *Earth and Planetary Science Letters*, v. 196, p. 17–33.
- Sturt, B.A., Pringle, I.R., and Ramsay, D.M., 1978, The Finnmarkian phase of the Caledonian Orogeny: *Journal of the Geological Society of London*, v. 135, p. 597–610.
- Thomas, W.A., and Astini, R.A., 2007, Vestiges of an Ordovician west-vergent thin skinned Ocoyic thrust belt in the Argentine Precordillera, Southern Central Andes: *Journal of Structural Geology*, v. 29, p. 1369–1385.

- Trotter, J.A., Williams, I.S., Barnes, C.R., Lécuyer, C., and Nicoll, R.S., 2008, Did cooling oceans trigger Ordovician biodiversification?: Evidence from conodont thermometry: *Science*, v. 321, p. 550–554.
- Vandenbroucke, T., Armstrong, H.A., Williams, A., Paris, F., Sabbe, K., Zalasiewicz, J., Nölvak, J., and Verniers, J., 2010, Epipelagic chitinozoan biotopes map a steep latitudinal temperature gradient for earliest Late Ordovician seas: Implication for a cooling Late Ordovician climate: *Palaeogeography, Palaeoclimatology, Palaeoecology*, v. 294, no. 3–4, p. 202–219.
- Veizer, J., Bruckschen, P., Pawellek, F., Diener, A., Podlaha, O.G., Carden, G.A.F., Jasper, T., Korte, C., Strauss, H., Azmy, K., and Ala, D., 1997, Oxygen isotope evolution of Phanerozoic seawater: *Palaeogeography, Palaeoclimatology, Palaeoecology*, v. 132, p. 159–172.
- Veizer, J., Ala, D., Azmy, K., Bruckschen, P., Buhl, D., Bruhn, F., Carden, G.A.F., Diener, A., Ebner, S., Goddard, Y., Jasper, T., Korte, C., Pawellek, F., Podlaha, O.G., and Strauss, H., 1999, $^{87}\text{Sr}/^{86}\text{Sr}$, ^{13}C , and ^{18}O evolution of Phanerozoic seawater: *Chemical Geology*, v. 161, p. 59–88.
- Veveers, J.J., 2004, Gondwanaland from 650–500 Ma assembly through 320 Ma merged in Pangea to 185–100 Ma breakup: Supercontinental tectonics via stratigraphy and radiometric dating: *Earth-Science Reviews*, v. 68, p. 1–132.
- Videt, B., Paris, F., Rubino, J.-L., Boumendjel, K., Dabard, M.-P., Loi, A., Ghienne, J.-F., Marante, A., and Gorini, A., 2010, Biostratigraphical calibration of third order Ordovician sequences on the northern Gondwana platform: *Palaeogeography, Palaeoclimatology, Palaeoecology*, v. 296, no. 3–4, p. 359–375.
- Walker, J.C.G., Hays, P.B., and Kasting, J.F., 1981, A negative feedback mechanism for the long-term stabilization of Earth's surface temperature: *Journal of Geophysical Research*, v. 86, p. 9776–9782.
- Wallmann, K., 2001a, Controls on the Cretaceous and Cenozoic evolution of seawater composition, atmospheric CO_2 , and climate: *Geochimica et Cosmochimica Acta*, v. 65, p. 3005–3025.
- Wallmann, K., 2001b, The geological water cycle and the evolution of marine $\delta^{18}\text{O}$ values: *Geochimica et Cosmochimica Acta*, v. 65, p. 2469–2485.
- Wellman, C.H., Osterloff, P.L., and Mohluddln, U., 2003, Fragments of the earliest land plants: *Nature*, v. 425, p. 282–285.
- Wenzel, B., Lécuyer, C., and Joachimski, M.M., 2000, Comparing oxygen isotope records of Silurian calcite and phosphate — $\delta^{18}\text{O}$ composition of brachiopods and conodonts: *Geochimica et Cosmochimica Acta*, v. 64, no. 11, p. 1859–1872.
- Yapp, C.J., and Poeths, H., 1996, Carbon isotopes in continental weathering environments and variations in ancient atmospheric CO_2 pressure: *Earth and Planetary Science Letters*, v. 137, p. 71–82.
- Young, S.A., Saltzman, M.R., Foland, K.A., Linder, J.S., and Kump, L.R., 2009, A major drop in seawater $^{87}\text{Sr}/^{86}\text{Sr}$ during the Middle Ordovician (Darriwilian): Links to volcanism and climate?: *Geology*, v. 37, p. 951–954.

MANUSCRIPT RECEIVED 5 JULY 2010

REVISED MANUSCRIPT RECEIVED 23 SEPTEMBER 2010

MANUSCRIPT ACCEPTED 23 SEPTEMBER 2010

Printed in the USA